Available online at www.sciencedirect.com
SCIENCE DIRECT
Composites: Part B 37 (2006) 10–20
composites Part B: engineering
www.elsevier.com/locate/compositesb

Static analysis of functionally graded elastic anisotropic plates using a discrete layer approach

Fernando Ramirez[a,*], Paul R. Heyliger[a], Ernian Pan[b]

[a]Department of Civil Engineering, Colorado State University, Fort Collins, CO 80523 USA
[b]Department of Civil Engineering, University of Akron, Akron, OH 44325, USA

Received 27 December 2004; revised 31 January 2005; accepted 16 May 2005

Abstract

An approximate solution for the static analysis of three-dimensional, anisotropic, elastic plates composed of functionally graded materials (FGM) is presented. The solution is obtained by using a discrete layer theory in combination with the Ritz method in which the plate is divided into an arbitrary number of homogeneous and/or FGM layers. Two types of functionally graded materials are considered: an exponential variation of the mechanical properties through the thickness of the plate, and mechanical properties as a function of the fiber orientation, which varies quadratically through the laminate thickness. The present approach is not dependent on a specific transition function, and any continuous function representing the variation of the material properties in the thickness direction may be incorporated in the model. The method is validated by solving the problem of a single simply supported FGM plate, for which excellent agreement with the exact solution is obtained. Two more examples with different boundary conditions and different material configurations are presented in order to demonstrate the applicability of this solution. Homogeneous, graded, and bi-layer plates are examined in order to study potential advantages of using FGM.

Keywords: A. Anisotropic; Composite plates

1. Introduction

Functionally graded materials (FGM) are characterized by a gradual change in properties within the specimen as a function of the position coordinates. The property gradient in the material is typically caused by a position-dependent chemical composition, microstructure or atomic order [1]. There are several studies about the processing of FGM, and an overview of the different manufacturing methods can be found in Kieback et al. [1]. There are two major groups of manufacturing methods. In the first class, known as constructive processes, the gradients are produced by selectively stacking two or more different materials. In the second class, known as transport based processes, transport phenomena is used to create compositional and microstructural gradients during the production of a component [2]. These manufacturing processes include: centrifugal casting, electrophoretic deposition, spark plasma sintering, and directed vapor deposition, among others [3–6].

FGM have been presented as an alternative to laminated composite materials that show a mismatch in properties at material interfaces. This material discontinuity in laminated composite materials leads to large interlaminar stresses and the possibility of initiation and propagation of cracks [7]. This problem is reduced in FGM because of the gradual change in mechanical properties as a function of position through the composite laminate. Numerous analyses of the behavior of cracks in FGM have been published [8–12].

Studies of the static and dynamic behavior of composite plates made of FGM have seen a smaller number of investigations. Reddy [7] presented Navier's solutions of rectangular plates, and finite element models based on the third-order shear deformation plate theory for the analysis of through-thickness functionally graded plates. The simply supported plates were proposed to have isotropic, two-constituent material distribution through the thickness, with the modulus of elasticity of the plate varying according to a power-law distribution in terms of the volume fractions of

* Corresponding author. Tel.: +1 970 4912801.
E-mail address: framirez@engr.colostate.edu (F. Ramirez).

1359-8368/$ - see front matter © 2005 Elsevier Ltd. All rights reserved.
doi:10.1016/j.compositesb.2005.05.009

the constituents. Cheng and Batra [13] studied the deflection of functionally graded plates using the first-order shear deformation theory (FSDT) and the higher-order shear deformation theory (HSDT), and its relationship to that of an equivalent homogeneous Kirchhoff plate. Cheng and Batra [14] also used Reddy's third-order plate theory to study buckling and steady state vibrations of a simply supported functionally gradient isotropic polygonal plate resting on a Winkler Pasternak elastic foundation and subjected to uniform in-plane hydrostatic loads. They later obtained a closed form solution for the thermo-mechanical deformations of an isotropic linear thermo-elastic functionally graded elliptic plate [15]. Vel and Batra [16,17] obtained exact solutions for three-dimensional deformations of a simply supported functionally graded rectangular plate subjected to mechanical and thermal loads, and for free and forced vibrations of simply supported functionally graded rectangular plates. In both of these studies, two-constituent metal–ceramic functionally graded rectangular plates were considered with a power-law through-the-thickness variation of the volume fractions of the constituents, with the effective material properties at a point estimated by either the Mori-Tanaka or self-consistent schemes. Sankar [18] obtained an elasticity solution for a functionally graded beam subjected to transverse loads, with the Young's modulus of the beam varying exponentially through the thickness, and the Poisson ratio held constant. Martin et al. [19] solved the problem of a point force acting in an unbounded, three-dimensional, elastic exponentially graded solid. Pan [20] presented an exact solution for three-dimensional, anisotropic, linearly elastic, and functionally graded rectangular composite laminates under simply supported edge conditions. The solution was expressed in terms of the pseudo-Stroh formalism, and the composite laminates can be made of multilayered functionally graded materials with their properties varying exponentially in the thickness direction.

In this study, the three-dimensional static analysis of functionally graded composites plates is considered using a discrete layer theory in combination with the Ritz method. Solutions to the weak form of the governing equations of equilibrium are obtained by using continuous functions to approximate the three displacement components within each layer. These functions are selected in such a way to separate their dependence on the thickness coordinate to that on the in-plane coordinates, allowing for the brake in the gradient of the displacements across a material interface and the potential corresponding discontinuity in the in-plane stresses. Two different types of through-thickness variation for the mechanical properties are considered. First, an exponential change of the elastic stiffness components as a function of the out-of-plane coordinate is studied ([18–20]), with its transition function directly incorporated into the governing equations. The second type of material gradient is obtained by considering a fiber-reinforced material in which the orientation of the fibers varies quadratically across the laminate thickness [21]. The proposed approach is validated by determining the displacements and stresses of a simply supported FGM plate subjected to a sinusoidal load for which the exact solution is known [20]. The discrete layer approximation is applied to solve two more examples: a rectangular plate under sinusoidal applied load with its four edges simply supported, and a rectangular plate subjected to the same load but with two opposite edges simply supported and the other two edges free. Each of these two examples is solved for a single homogeneous graphite/epoxy plate, a graphite/epoxy plate with the fibers oriented in the y-direction on the bottom surface of the laminate and smoothly changing through the thickness to be oriented in the x-direction on the top surface, and a two-layer plate with the bottom layer having the fibers oriented in the y-direction, and oriented in the x-direction on the top layer.

The solution approach presented here is not dependent on a specific transition function describing the gradation of the mechanical properties of the material. Any continuous function representing the variation of the material properties as a function of the position coordinates may be incorporated into the present solution, and a similar level of accuracy is expected to be obtained. Additionally, the approach presented here is not dependent on specific edge boundary conditions, and it becomes an excellent alternative to the more complex and restrictive exact solution approaches, which are limited to very specific sets of boundary conditions.

2. Theory

2.1. Geometry and mechanical properties gradation

A conventional rectangular Cartesian coordinate system, with its origin located at the lower left corner of the laminate, is used to describe the deformation of the rectangular plates. The thickness direction is coincident with the z-coordinate axis, and the x and y-axes are coincident with the planar directions of the plate. The total thickness of the plate is H, and the corresponding horizontal dimensions are L_x and L_y. Layered rectangular plates composed of an arbitrary number of elastic homogeneous or functionally graded elastic layers N, with perfect bonding along interfaces, are considered. Each layer has individual layer thickness h_i, where h_1 corresponds to the bottom layer, and h_N to the top layer.

For the case in which the variation of the material properties is exponential in the z-direction, the components of the elastic stiffness tensor can be expressed as

$$C_{ik}(z) = C^0_{ik} e^{\eta z} \tag{1}$$

where C_{ik} are the components of the stiffness tensor at any height z, C^0_{ik} are the components at $z=0$, and η is the exponential factor characterizing the degree of the material

gradient in the z-direction. Note that η has units $[1/L]$, and $\eta=0$ corresponds to a homogeneous material [20].

2.2. Governing equations

Considering the through-thickness gradation of the components of the elastic stiffness tensor, the constitutive equations for each anisotropic, linearly elastic layer in the laminate can be written as:

$$\sigma_i = C^0_{ik} e^{\eta z} \gamma_k \tag{2}$$

where σ_i and γ_k denote the components of the stress and strain fields, respectively, and the standard contracted engineering notation is used.

The components of the rotated elastic stiffness tensor for an orthotropic material are given in matrix form as

$$[C] = \begin{bmatrix} C_{11} & C_{12} & C_{13} & 0 & 0 & C_{16} \\ C_{12} & C_{22} & C_{23} & 0 & 0 & C_{26} \\ C_{13} & C_{23} & C_{33} & 0 & 0 & C_{36} \\ 0 & 0 & 0 & C_{44} & C_{45} & 0 \\ 0 & 0 & 0 & C_{45} & C_{55} & 0 \\ C_{16} & C_{26} & C_{36} & 0 & 0 & C_{66} \end{bmatrix} \tag{3}$$

The components of the strain field γ_{ij} are related to the displacement field u_i by the relation

$$\gamma_{ij} = \frac{1}{2}\left(\frac{\partial u_i}{\partial x_j} + \frac{\partial u_j}{\partial x_i}\right) \tag{4}$$

The equations of equilibrium in the absence of body forces are given by

$$\sigma_{ij,j} = 0 \tag{5}$$

2.3. Variational formulation

Following the standard variational method of approximation (Reddy [22]), we multiply the equations of motion by the first variation of the displacements, and then integrate the result over the volume of the domain and set the result equal to zero, resulting in

$$\int_V \delta u_i \sigma_{ij,j} \mathrm{d}V = 0 \tag{6}$$

Integrating this equations by parts and applying the divergence theorem yields the final weak form of the governing equations which represent the principle of virtual work in the absence of body forces.

$$\int_V \sigma_{ij} \delta \gamma_{ij} \mathrm{d}V - \oint_S \sigma_{ij} n_j \delta u_i \mathrm{d}S = 0 \tag{7}$$

Substituting the constitutive equations into the final weak form yields the following expression which includes the transition function describing the through-thickness variation of the components of the elastic stiffness tensor:

$$\begin{aligned} 0 = \int_V e^{\eta z} \Bigg\{ & \left[C^0_{11}\frac{\partial u}{\partial x} + C^0_{12}\frac{\partial v}{\partial y} + C^0_{13}\frac{\partial w}{\partial z} + C^0_{16}\left(\frac{\partial v}{\partial x} + \frac{\partial u}{\partial y}\right)\right]\frac{\partial \delta u}{\partial x} \\ & + \left[C^0_{12}\frac{\partial u}{\partial x} + C^0_{22}\frac{\partial v}{\partial y} + C^0_{23}\frac{\partial w}{\partial z} + C^0_{26}\left(\frac{\partial v}{\partial x} + \frac{\partial u}{\partial y}\right)\right]\frac{\partial \delta v}{\partial y} \\ & + \left[C^0_{13}\frac{\partial u}{\partial x} + C^0_{23}\frac{\partial v}{\partial y} + C^0_{33}\frac{\partial w}{\partial z} + C^0_{36}\left(\frac{\partial v}{\partial x} + \frac{\partial u}{\partial y}\right)\right]\frac{\partial \delta w}{\partial z} \\ & + \left[C^0_{44}\left(\frac{\partial v}{\partial z} + \frac{\partial w}{\partial y}\right) + C^0_{45}\left(\frac{\partial u}{\partial z} + \frac{\partial w}{\partial x}\right)\right]\left(\frac{\partial \delta v}{\partial z} + \frac{\partial \delta w}{\partial y}\right) \\ & + \left[C^0_{55}\left(\frac{\partial u}{\partial z} + \frac{\partial w}{\partial x}\right) + C^0_{45}\left(\frac{\partial v}{\partial z} + \frac{\partial w}{\partial y}\right)\right]\left(\frac{\partial \delta u}{\partial z} + \frac{\partial \delta w}{\partial x}\right) \\ & + \left[C^0_{16}\frac{\partial u}{\partial x} + C^0_{26}\frac{\partial v}{\partial y} + C^0_{36}\frac{\partial w}{\partial z} + C^0_{66}\left(\frac{\partial v}{\partial x} + \frac{\partial u}{\partial y}\right)\right] \\ & \times \left(\frac{\partial \delta v}{\partial x} + \frac{\partial \delta u}{\partial y}\right)\Bigg\} \mathrm{d}V - \oint_s (t_x \delta u + t_y \delta v + t_z \delta z) \mathrm{d}S \end{aligned} \tag{8}$$

where u, v, and w represent the displacement components in the x, y, and z-directions, respectively, and t_x, t_y, and t_z the traction components. This equation results in three different equations of equilibrium when the coefficients of the variations of the displacements are collected.

2.4. Discrete-layer approximation and solution

The displacements u_i are approximated by a finite linear combination of functions that must satisfy the boundary conditions and be continuous as required by the variational principle. Approximations to the three displacements are generated in terms of the global (x, y, z) coordinates. In this study, the approximations for each displacement component are constructed in such a way as to separate the dependence in the plane with that in the direction perpendicular to the interface. Hence approximations for the three unknown displacements are sought in the form

$$\begin{aligned} u(x,y,z) &= \sum_{i=1}^{m}\sum_{j=1}^{n} U_{ij} \Gamma^u_i(x,y) \Phi^u_j(z), \\ v(x,y,z) &= \sum_{i=1}^{m}\sum_{j=1}^{n} V_{ij} \Gamma^v_i(x,y) \Phi^v_j(z), \\ w(x,y,z) &= \sum_{i=1}^{m}\sum_{j=1}^{n} W_{ij} \Gamma^w_i(x,y) \Phi^w_j(z) \end{aligned} \tag{9}$$

Where, the elements U_{ij}, V_{ij}, and W_{ij} are the approximation coefficients associated with the jth layer of the discretized laminate corresponding to the ith term of the in-plane approximation function for each of the displacement variables. In the thickness direction, one-dimensional Lagrangian interpolation polynomials are used for $\Phi_j(z)$

for each variable, while for the in-plane functions $\Gamma_i(x, y)$, different types of approximations can be used being power and Fourier series the most commonly selected.

Substitution of these approximation functions into Eq. (8), collecting the coefficients of the variations of the displacements, integrating with respect to the thickness coordinate z, and placing the results in matrix form yields the result

$$\begin{bmatrix} [K^{uu}] & [K^{uv}] & [K^{uw}] \\ [K^{vu}] & [K^{vv}] & [K^{vw}] \\ [K^{wu}] & [K^{wv}] & [K^{ww}] \end{bmatrix} \begin{Bmatrix} \{u\} \\ \{v\} \\ \{w\} \end{Bmatrix} = \begin{Bmatrix} \{f^u\} \\ \{f^v\} \\ \{f^w\} \end{Bmatrix} \tag{10}$$

Here the sub-matrices $[K]$ contain the elements of the stiffness matrix, the vectors $\{u\}\cdot\{v\}$, and $\{w\}$ are the corresponding approximation coefficients U_{ij}, V_{ij}, and W_{ij} of Eq. (9), and the vectors $\{f^u\}$, $\{f^v\}$, and $\{f^w\}$ represent the external loading acting on the plate in each of the coordinate directions.

The elements of each of the sub-matrices $[K]$ have a specific form as a result of the pre-integration with respect to the thickness coordinate. They consist of the product of the thickness approximation functions and the gradient function, fully integrated, and then multiplied by the in-plane approximations. The matrix Eq. (10) is solved for the coefficients of the approximation functions, which are then used to determine the displacements and stresses at any location within the laminated plate.

In order to illustrate the pre-integration with respect to the thickness coordinate, we consider the sub-matrix $[K^{uu}]$ given by

$$K^{uu} = \int_V e^{\eta z}\left[C_{11}^0 \frac{\partial u}{\partial x}\frac{\partial u}{\partial x} + C_{16}^0\left(\frac{\partial u}{\partial y}\frac{\partial u}{\partial x} + \frac{\partial u}{\partial x}\frac{\partial u}{\partial y}\right) + C_{55}^0 \frac{\partial u}{\partial z}\frac{\partial u}{\partial z} + C_{66}^0 \frac{\partial u}{\partial y}\frac{\partial u}{\partial y}\right] dV \tag{11}$$

Substituting the approximation functions (9) in Eq. (11), its first term becomes

$$\int_V C_{11}^0 e^{\eta z}\left(\sum_{i=1}^{m}\sum_{\alpha=1}^{N+1}\frac{\partial \Gamma_i^u(x,y)}{\partial x}\Phi_\alpha^u(z)\right)\left(\sum_{j=1}^{m}\sum_{\beta=1}^{N+1}\frac{\partial \Gamma_j^u(x,y)}{\partial x}\Phi_\beta^u(z)\right) dV \tag{12}$$

Where, m is the number of terms in the in-plane approximation functions, and N is the total number of layers in the laminate. Note that the summations for α and β extend to $(N+1)$ which is the number of layer interfaces in the laminated plate and the number of approximation functions in the thickness direction. Expression (12) can be re-written as

$$\int_0^H C_{11}^0 e^{\eta z}\sum_{\alpha=1}^{N+1}\sum_{\beta=1}^{N+1}\Phi_\alpha^u(z)\Phi_\beta^u(z)dz \times \int_0^{L_x}\int_0^{L_y}\sum_{i=1}^{m}\sum_{j=1}^{m}\frac{\partial \Gamma_i^u(x,y)}{\partial x}\frac{\partial \Gamma_j^u(x,y)}{\partial x}dxdy \tag{13}$$

and with the first integral termed as $A_{\alpha\beta}$, expression (13) can be written as

$$A_{\alpha\beta}\int_0^{L_x}\int_0^{L_y}\sum_{i=1}^{m}\sum_{j=1}^{m}\frac{\partial \Gamma_i^u(x,y)}{\partial x}\frac{\partial \Gamma_j^u(x,y)}{\partial x}dxdy \tag{14}$$

The linear Lagrangian interpolation functions used in the thickness direction are defined as [23]

$$\Phi_1(z) = 1 - \frac{z - z_1}{z_2 - z_1}, \quad z_1 \le z \le z_2 \tag{15}$$

$$\Phi_k(z) = \frac{z - z_{k-1}}{z_k - z_{k-1}}, \quad z_{k-1} \le z \le z_k \tag{16}$$

$$\Phi_k(z) = 1 - \frac{z - z_k}{z_{k+1} - z_k}, \quad z_k \le z \le z_{k+1} \tag{17}$$

$$\Phi_{N+1}(z) = \frac{z - z_n}{z_{n+1} - z_n}, \quad z_n \le z \le z_{n+1} \tag{18}$$

where z_k are the coordinates of the top and bottom surfaces of each discrete layer. Note that the sum over the number of layers of the laminate in expression (14) is limited to the layers over which the functions $\Gamma_k(z)$ are defined. These functions are defined at the most over two adjacent layers [24].

Substituting Eqs. (15)–(18) into expression (14), the first element of the matrix $A_{\alpha\beta}$ is given by

$$A_{11} = \int_{z_1}^{z_2} C_{11}^0 e^{\eta z}\left(1 - \frac{z - z_1}{z_2 - z_1}\right)^2 dz \tag{19}$$

After integration it becomes

$$A_{11} = C_{11}^0\left\{\frac{[2\eta^2 z_2 z_1 - 2\eta(z_2 - z_1) - \eta^2(z_2^2 + z_1^2) - 2]e^{\eta z_1} + 2e^{\eta z_2}}{\eta^3(z_1 - z_2)^2}\right\} \tag{20}$$

Where, z_1 and z_2 are the thickness coordinates of the bottom and top surfaces respectively of the corresponding layer. It is important to realize that the form of the pre-integrated elements of the sub-matrices depends on the transition function describing the gradient of the material properties through the thickness of the laminate. Furthermore, any continuous transition function may be implemented in the present discrete layer approach. The pre-integration in the thickness direction and the inclusion of the gradation function into the governing equations do not alter the symmetry of the global stiffness matrix.

3. Numerical examples

Three examples are considered in this section. First, a single orthotropic FGM plate, with known exact solution [20] is examined in order to validate the approximate model presented here. This model has also been successfully applied in the past for the static and free vibration analysis of laminated plates composed of homogeneous ($\eta=0$) elastic, piezoelectric or magnetostrictive layers [25,26]. Two more plates made of graphite/epoxy are considered with the following boundary conditions: four edges simply supported (SSSS), and two opposite edges simply supported and the other two free (SSFF).

3.1. FGM simply supported plate

The first example considered is a single-layer exponentially graded orthotropic plate made of a material with components of the elastic stiffness tensor given by [20]

$$[C]=\begin{bmatrix} 7.3802 & 2.3121 & 1.8682 & 0 & 0 & 0 \\ 2.3121 & 173.406 & 2.3121 & 0 & 0 & 0 \\ 1.8682 & 2.3121 & 7.3802 & 0 & 0 & 0 \\ 0 & 0 & 0 & 3.445 & 0 & 0 \\ 0 & 0 & 0 & 0 & 1.378 & 0 \\ 0 & 0 & 0 & 0 & 0 & 3.445 \end{bmatrix} e^{\eta z}\, 10^9\ \mathrm{N/m^2} \tag{21}$$

The dimensions of the plate are $L_x=L_y=3.0$ m, and $H=1.0$ m. The loading is a normal traction in the positive z-direction acting on the upper face of the laminate that has the form:

$$t_z(x,y)=\sin\left(\frac{\pi x}{L_x}\right)\sin\left(\frac{\pi y}{L_y}\right) \tag{22}$$

All the other tractions on the top and bottom surfaces of the laminate are zero. The edge boundary conditions are consistent with those of simple support. Hence, $\sigma_{xx}=0$, $v=w=0$ at $x=0$ and $x=L_x$, and $\sigma_{yy}=0$, $u=w=0$ at $y=0$ and $y=L_y$. The in-plane approximation functions, satisfying these boundary conditions, for each of the three displacements are in the form:

$$\Gamma_j^u(x,y)=\cos px\sin qy \tag{23}$$

$$\Gamma_j^v(x,y)=\sin px\cos qy \tag{24}$$

$$\Gamma_j^w(x,y)=\sin px\sin py \tag{25}$$

where $p=n\pi/L_x$ and $q=m\pi/L_x$. Only one term is required to match the exact solution. Here the index j is a single integer that is linked to the numbers used for p and q in each of the terms of the approximation functions.

The plate is discretized into 30 individual layers, and analyses are performed considering five different values for the exponential factor describing the gradient of the material properties in the z-direction. They are $\eta=-1.0$, -0.5, 0.0, 0.5, and 1.0. Displacements and stresses are determined at different locations through the thickness of the laminate with the (x, y) coordinates fixed at $(0.75L_x, 0.75L_y)$. Results are shown in Table 1 and Fig. 1, along with the exact solution presented by Pan [20]. Excellent agreement is obtained.

This problem was also solved by dividing the laminate into homogeneous layers, each layer having elastic constants given by the average of the mechanical properties within the respective layer, and calculated as

$$(C_{ij})_k=\int_{z_o}^{z_f} C_{ij}^0\frac{e^z}{h_k}\mathrm{d}z \tag{26}$$

where z_0, z_f, and h_k are the coordinate of the lower face, upper face, and the layer thickness, respectively. Results for displacements are shown in Table 1 where 20 discrete homogeneous layers are used, and it can be seen that a maximum error of 2.0% is obtained (in-plane displacement u at the mid-plane of the plate) when compared to the exact solution. This result indicates that it may not be necessary to include the transition function into the governing equations to obtain acceptable results when discrete layer models are applied to functionally graded laminates.

3.2. Graphite-epoxy plates

The following two examples involve plates composed of graphite/epoxy in which the elastic constants in tensor form are given below for the case when the fibers are oriented parallel to the y-axis.

$$[C]=\begin{bmatrix} 11.662 & 4.363 & 3.918 & 0 & 0 & 0 \\ 4.363 & 183.443 & 4.363 & 0 & 0 & 0 \\ 3.918 & 4.363 & 11.662 & 0 & 0 & 0 \\ 0 & 0 & 0 & 7.170 & 0 & 0 \\ 0 & 0 & 0 & 0 & 2.870 & 0 \\ 0 & 0 & 0 & 0 & 0 & 7.170 \end{bmatrix} 10^9\ \mathrm{N/m^2} \tag{27}$$

For each of these examples three different material configurations are analyzed:

- A homogeneous plate with the material properties given by Eq. (27).
- A functionally graded plate with through-thickness variation of the mechanical properties that vary with the orientation of the fibers. The orientation of the fibers is assumed to vary as a function of the thickness coordinate, being oriented in the y-direction on the bottom surface, and in the x-direction on the top surface of the plate. Materials having this configuration can be manufactured by stacking thin layers having different

Table 1
Displacements (10^{-11})m, and stresses (N/m^2) at ($0.75L_x$, $0.75L_y$) for the exponentially graded simply supported plate

		z=0.0			z=0.5			z=1.0		
	η	30 D.L.	Exact	20 H.D.L.	30 D.L.	Exact	20 H.D.L.	30 D.L.	Exact	20 H.D.L.
u	−1.0	6.487	6.488	6.476	0.125	0.125	0.127	−7.091	−7.092	−7.063
	−0.5	5.465	5.465	5.453	0.475	0.475	0.476	−5.327	−5.328	−5.308
	0.0	4.549	4.549	4.538	0.673	0.673	0.674	−3.949	−3.949	−3.937
	0.5	3.740	3.740	3.730	0.757	0.757	0.757	−2.890	−2.890	−2.882
	1.0	3.036	3.036	3.027	0.761	0.761	0.760	−2.089	−2.089	−2.084
v	−1.0	2.684	2.685	2.669	−0.209	−0.209	−0.209	−3.642	−3.643	−3.604
	−0.5	2.193	2.194	2.178	−0.035	−0.035	−0.035	−2.758	−2.759	−2.732
	0.0	1.773	1.774	1.759	0.076	0.076	0.076	−2.073	−2.073	−2.056
	0.5	1.418	1.419	1.406	0.140	0.140	0.140	−1.545	−1.545	−1.534
	1.0	1.123	1.123	1.112	0.170	0.170	0.170	−1.142	−1.142	−1.135
w	−1.0	21.132	21.134	21.086	22.755	22.757	22.709	28.409	28.412	28.355
	−0.5	16.723	16.725	16.686	18.022	18.024	17.986	21.731	21.732	21.690
	0.0	13.094	13.095	13.065	14.128	14.129	14.100	16.567	16.568	16.536
	0.5	10.143	10.144	10.121	10.960	10.961	10.939	12.569	12.570	12.547
	1.0	7.774	7.775	7.757	8.415	8.415	8.400	9.480	9.481	9.464
σ_{xx}	−1.0	−0.517	−0.518	−0.510	0.068	0.068	0.069	0.339	0.340	0.338
	−0.5	−0.435	−0.435	−0.430	0.040	0.040	0.040	0.390	0.391	0.388
	0.0	−0.361	−0.361	−0.358	0.011	0.011	0.011	0.450	0.450	0.446
	0.5	−0.296	−0.296	−0.294	−0.018	−0.018	−0.190	0.517	0.517	0.511
	1.0	−0.240	−0.240	−0.239	−0.046	−0.046	−0.047	0.593	0.593	0.584
σ_{yy}	−1.0	−4.962	−4.973	−4.759	0.317	0.317	0.318	2.624	2.627	2.557
	−0.5	−4.058	−4.066	−3.912	0.125	0.125	0.125	3.236	3.241	3.142
	0.0	−3.284	−3.290	−3.180	−0.074	−0.074	−0.075	3.970	3.977	3.840
	0.5	−2.630	−2.634	−2.556	−0.273	−0.273	−0.276	4.840	4.850	4.661
	1.0	−2.084	−2.086	−2.032	−0.467	−0.467	−0.471	5.859	5.872	5.614
σ_{zz}	−1.0	0.000	0.000	0.000	0.283	0.283	0.283	0.500	0.500	0.500
	−0.5	0.000	0.000	0.000	0.262	0.262	0.262	0.500	0.500	0.500
	0.0	0.000	0.000	0.000	0.241	0.241	0.240	0.500	0.500	0.500
	0.5	0.000	0.000	0.000	0.219	0.219	0.219	0.500	0.500	0.500
	1.0	0.000	0.000	0.000	0.198	0.198	0.197	0.500	0.500	0.500

Here, D.L. stands for discrete layers, and H.D.L. stands for homogeneous discrete layers.

orientations [21]. The orientation of the fibers measured with respect to the y-axis is expressed as

$$\theta(z) = \frac{\pi}{2}\left(\frac{z}{H}\right)^2 \tag{28}$$

This problem is solved by using the approach presented at the end of the previous example in which the laminate is divided into homogeneous layers. The elastic stiffness constants for each layer are obtained by tensor transformation using the average fiber orientation obtained using Eq. (29):

$$\bar{\theta} = \int_{z_0}^{z_f} \frac{\pi}{2(z_f - z_0)}\left(\frac{z}{H}\right)^2 \mathrm{d}z = \frac{\pi(z_f^3 - z_o^3)}{6H^2(z_f - z_0)} \tag{29}$$

The through-thickness variation of some of the components of the elastic stiffness tensor is shown in Fig. 2. Note that as the fiber orientation changes the elements C_{16}, C_{26}, C_{36}, and C_{45} become nonzero.

- A two-layer plate with the bottom layer having the fibers oriented in y-direction, the top layer fibers in the x-direction, and with equal layer thickness used for each lamina is presented.

The laminate dimensions for all the examples are $L_x = 1.0$ m, $L_y = 2.0$ m, and total thickness $H = 0.20$ m.

3.2.1. SSSS graphite-epoxy plate

In this example a simply supported plate subjected to the sinusoidal traction of Eq. (22) acting on its top face and with its bottom face being traction free is considered. The boundary conditions at the edges are the same as those presented in the first example, and correspond to simple supports along the four edges of the laminate. Eqs. (23)–(25) are used as approximations, and only one term is required to obtained the exact solution. The plate is divided into a sequentially higher number of layers starting with 12 until convergence is obtained when 30 layers are used. Use of a higher number of layers resulted in changes in displacements and stresses smaller than 0.1%. This convergence criterion was applied for all the remaining examples.

Results are presented in Table 2 for the graded configuration case when 12, 16, 20, and 30 (converged) layers are used. For the homogeneous and bi-layer configurations only converged results are shown.

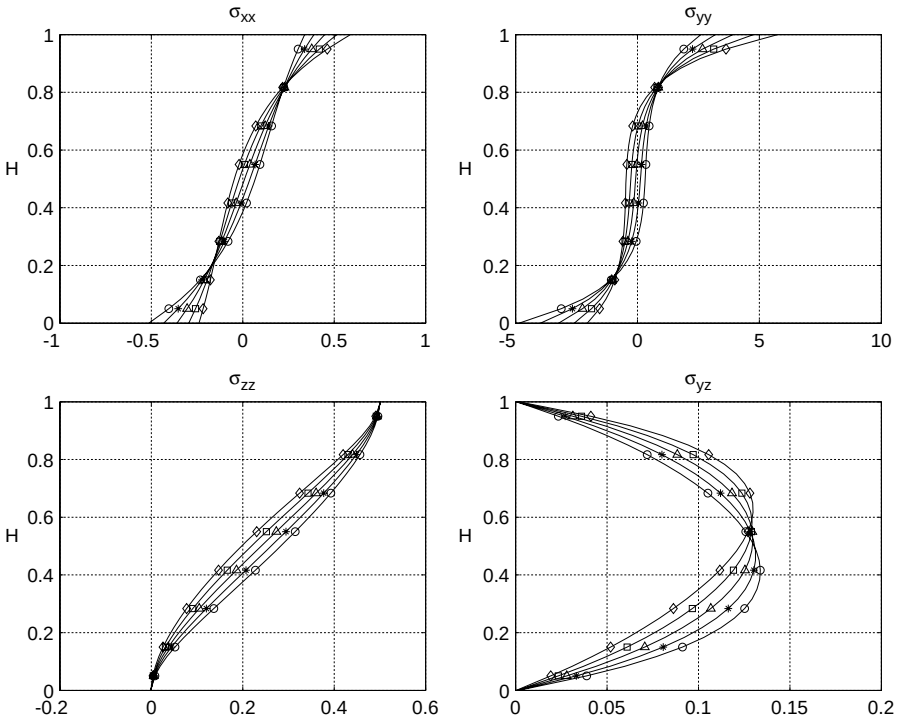

Fig. 1. Through-thickness variation of stress (N/m^2) for the exponentially graded plate. Solid lines represent the exact solution, whereas open circles indicate the D.L. solution for $\eta=1$, stars for $\eta=2$, open triangles for $\eta=3$, open squares for $\eta=4$, and open diamonds for $\eta=5$.

Through-thickness distribution of stresses can also be seen in Fig. 3 for the three material configurations mentioned in Section 3.2. Displacements and stresses shown in Table 2, as well as the stresses shown in Fig. 3 were calculated at different locations in the thickness direction, at the following (x, y) coordinates: u at $(0, L_y/2)$, v at $(L_x/2, 0)$, w, σ_{xx}, σ_{yy}, and σ_{zz} at $(L_x/2, L_y/2)$, and σ_{yz}, σ_{xz}, and σ_{xy} at $(L_x/4, L_y/4)$.

When 20 discrete layers are used to represent the graded plate, a maximum error of 5% relative to the converged

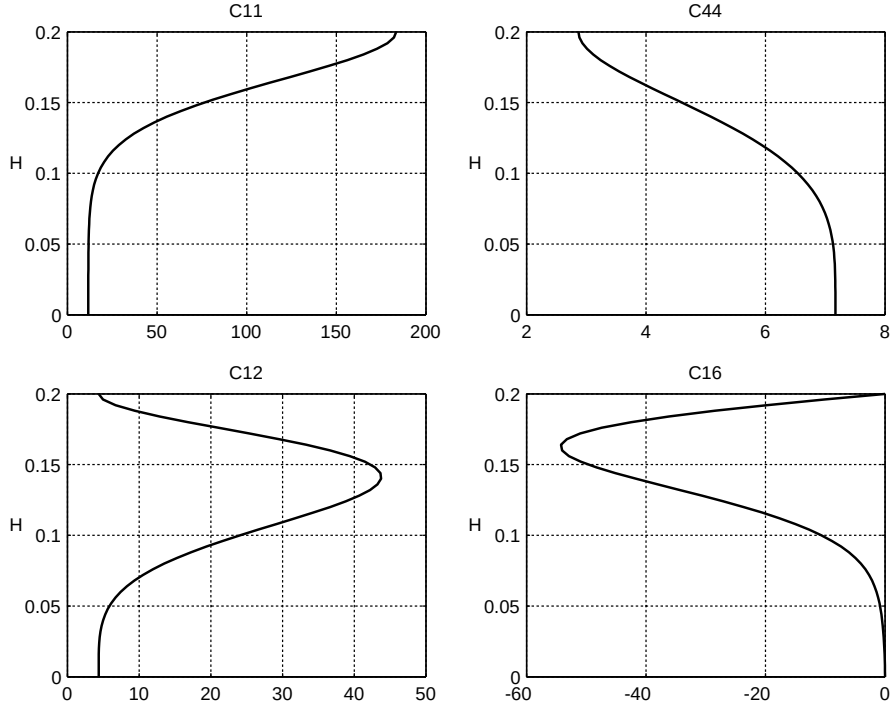

Fig. 2. Through-thickness variation of mechanical properties (GPa) for the graphite/epoxy plate.

Table 2
Displacements (10^{-10})m, and stresses (N/m^2) for the SSSS graphite/epoxy plate

	z	12 H.D.L.	16 H.D.L.	20 H.D.L.	30 H.D.L.	Bi-Layer	Homog.
u	0.00	1.815	1.821	1.824	1.828	1.477	1.754
	0.10	0.703	0.706	0.707	0.709	0.446	0.046
	0.20	−0.437	−0.438	−0.438	−0.438	−0.558	−1.677
v	0.00	0.358	0.359	0.359	0.360	0.300	0.779
	0.10	−0.230	−0.231	−0.231	−0.232	−0.258	0.003
	0.20	−0.792	−0.796	−0.798	−0.800	−0.779	−0.781
w	0.00	4.399	4.411	4.416	4.423	3.976	6.253
	0.10	4.545	4.557	4.562	4.569	4.086	6.382
	0.20	4.600	4.612	4.618	4.625	4.113	6.348
σ_{xx}	0.00	−6.046	−6.074	−6.087	−6.104	−4.933	−6.050
	0.20	24.841	25.431	25.640	25.795	32.460	6.135
σ_{yy}	0.00	−11.807	−11.874	−11.903	−11.940	−9.890	−23.802
	0.20	1.927	1.860	1.871	1.963	2.108	24.153
σ_{zz}	0.10	0.409	0.410	0.411	0.412	0.302	0.425
σ_{yz}	0.10	0.268	0.267	0.267	0.267	0.276	1.157
σ_{xz}	0.10	0.657	0.656	0.655	0.654	0.589	0.599
σ_{xy}	0.00	1.392	1.409	1.418	1.431	1.168	1.862
	0.20	−1.742	−1.429	−1.302	−1.170	−1.189	−1.821

Here, H.D.L. stands for homogeneous discrete layers, Bi-layer for two-layer laminate, and Homog. for single-layer homogeneous laminate.

values is obtained. Higher accuracy is expected as the number of layers is increased, or for the same number of layers when the gradient of the material properties is smoother. As seen in Fig. 3, there is an important discontinuity of in-plane stresses σ_{xx} and σ_{yy} for the bi-layer plate at the dissimilar layer caused by the difference in material properties and displacement gradients across the interface. Comparing the three different material configurations, the out-of-plane displacement w is reduced by about 35% for the bi-layer case and about 25% for the graded material in comparison to the homogenous plate. Additionally, the graded and bi-layer materials exhibit comparable

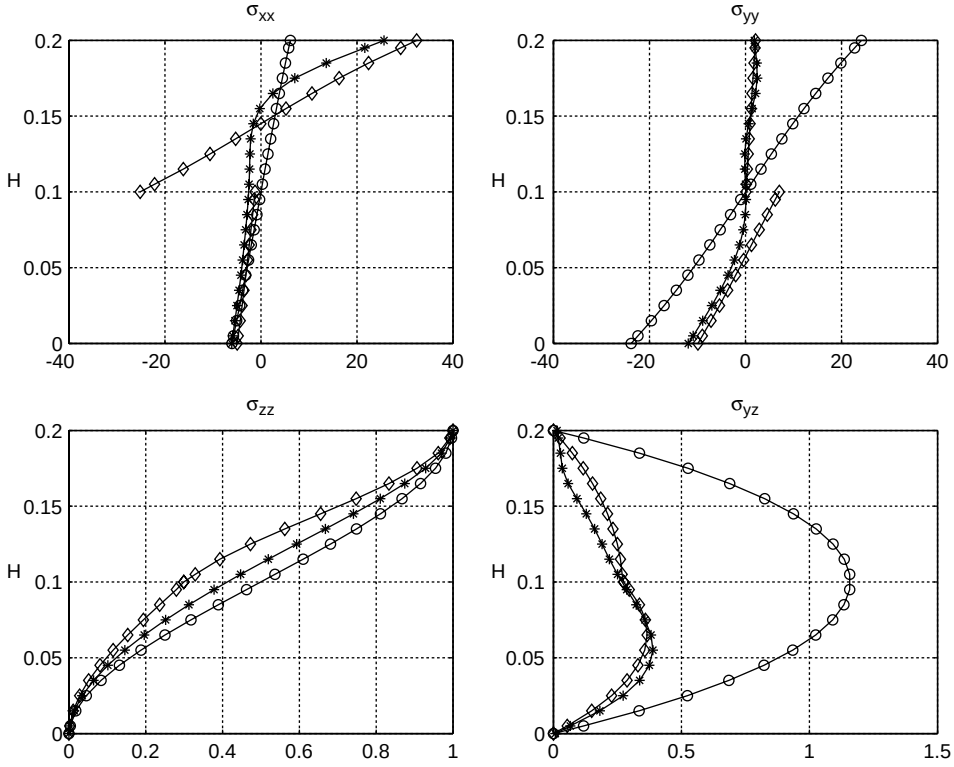

Fig. 3. Through-thickness variation of stress (N/m^2) for the SSSS graphite/epoxy plate. Open circles indicate single homogeneous plate, stars the graded plate, and open diamonds represent the two-layer laminate.

Table 3
Displacements (10^{-10})m, and stresses (N/m^2) for the SSFF graphite/epoxy plate

	z	12 H.D.L.	16 H.D.L.	20 H.D.L.	30 H.D.L.	Bi-Layer	Homog.
u	0.00	0.316	0.321	0.323	0.325	0.484	0.564
	0.10	0.256	0.258	0.259	0.260	0.214	0.046
	0.20	−0.024	−0.025	−0.025	−0.025	−0.155	−0.487
v	0.00	1.091	1.092	1.092	1.092	1.297	1.100
	0.10	−0.447	−0.450	−0.451	−0.452	−0.828	0.003
	0.20	−2.023	−2.030	−2.033	−2.035	−2.943	−1.102
w	0.00	11.220	11.257	11.274	11.292	14.784	8.578
	0.10	11.303	11.340	11.358	11.375	14.865	8.670
	0.20	11.322	11.359	11.377	11.394	14.833	8.673
σ_{xx}	0.00	−2.485	−2.571	−2.621	−2.682	−3.088	−3.358
	0.20	6.338	6.724	6.914	7.111	15.150	3.443
σ_{yy}	0.00	−31.781	−31.886	−31.898	−31.991	−37.749	−32.222
	0.20	3.685	3.703	3.714	3.729	5.338	32.577
σ_{zz}	0.10	0.575	0.560	0.512	0.512	0.413	0.499
σ_{yz}	0.10	1.235	1.259	1.326	1.321	0.979	1.678
σ_{xz}	0.10	0.054	0.047	0.027	0.030	0.429	0.471
σ_{xy}	0.00	0.860	0.639	0.532	0.412	0.222	0.872
	0.20	−1.068	−1.144	−1.178	−1.202	−1.710	−0.830

Here, H.D.L. stands for homogeneous discrete layers, Bi-layer for two-layer laminate, and Homog. for single-layer homogeneous laminate.

shear stresses and normal in-plane stress σ_{xx}, while σ_{yy} in the graded plate is about 20% smaller than that of the bi-layer plate. These results clearly show that for the specific conditions of this example, the graded laminate exhibits structural appealing traits compared to the bi-layer and homogeneous plate configurations.

3.2.2. SSFF graphite-epoxy plate

As a final example, a plate with different boundary conditions is studied. In this case, the laminate is simply supported along two opposites edges at $y=0$ and $y=L_y$, and the other two edges at $x=0$ and $x=L_x$ are free. The conditions at the top and bottom surfaces are the same as

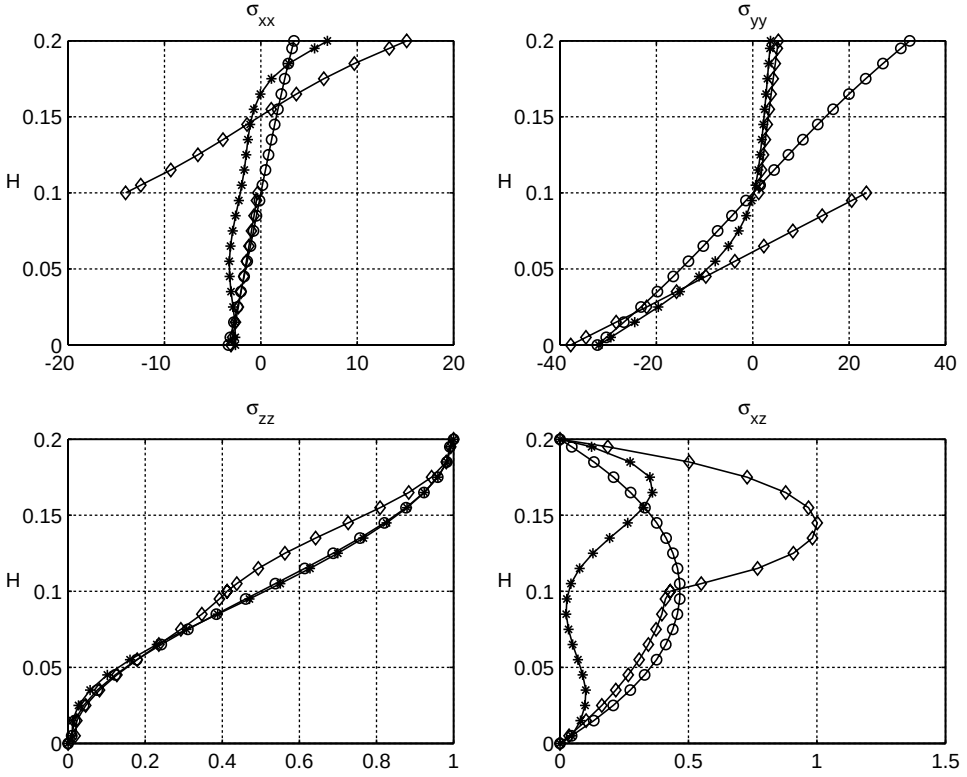

Fig. 4. Through-thickness variation of stress (N/m^2) for the SSFF graphite/epoxy plate. Open circles indicate single homogeneous plate, stars the graded plate, and open diamonds represent the two-layer laminate.

in the previous example, that is, the traction defined in Eq. (22) acting on the top of the plate is the only force considered. We include this example to show that this model is not restricted to the case of simple supports.

In order to satisfy the support conditions, power series are used for the approximation functions of the three displacements. They are given by

$$\Gamma_j^u(x,y) = (x - L_x/2)^n [y(y - L_y)]^{(m+1)} \quad n,m = 0,1,2,3,\ldots \tag{30}$$

$$\Gamma_j^v(x,y) = [x(x - L_x)]^{(n+1)} (y - L_y/2)^m \quad n,m = 0,1,2,3,\ldots \tag{31}$$

$$\Gamma_j^w(x,y) = (x - L_x/2)^n [y(y - L_y)]^{(m+1)} \quad n,m = 0,1,2,3,\ldots \tag{32}$$

Analyses are performed for an increasing number of layers and terms in the approximation functions, achieving convergence for 30 layers and $m=n=8$. Results are reported in Table 3 and Fig. 4, with displacements and stresses computed at the same locations as in the SSSS graphite/epoxy plate.

Analysis of results indicates that for the case in which the laminate is discretized into 20 homogeneous layers, the maximum error for the graded plate relative to converged values is smaller than 5%, showing again that the present approach gives acceptable results even without including the transition function describing the variation of the material properties in the solution of the governing equations. As expected for these boundary conditions, the homogeneous plate has smaller vertical displacements than the graded and bi-layer laminates because the fibers are oriented in the same direction in which the loads are carried to the supports through the entire thickness of the laminate. The magnitude of the shear stresses is of the same order for the three different material configurations, and the homogeneous case resulted in smaller or comparable maximum normal stresses. For these specific boundary conditions, the gradient of material properties employed in this example does not improve the performance of the laminate when compared to the homogeneous plate behavior.

4. Conclusions

A discrete layer model has been presented for the static analysis of functionally graded plates. The model allows the direct inclusion of the transition function describing the gradation of the mechanical properties into the governing equations. Validation of the present solution was obtained by comparing, with excellent agreement, the behavior of a simply supported plate made of an exponentially graded material with the exact solution derived by Pan [20]. Examples involving different boundary conditions (SSSS and SSFF), and material configurations, homogeneous, graded, and bi-layer laminates, were considered in order to demonstrate the applicability of the method. The primary features of and general conclusions obtained from this work can be summarized as follows:

1. The developed discrete layer approach can be successfully applied to the static analysis of plates made of materials in which the mechanical properties are functions of the position coordinates by direct incorporation of the transition functions into the governing equations.
2. Any continuous function describing the gradient of the elastic properties of the materials can be used along with the present approach for the static analysis of plates.
3. The present method can be applied to FGM plates by dividing the laminate into discrete homogeneous layers with mechanical properties obtained as the average values for the corresponding layer. The accuracy of the results will depend on the number of layers used in the analysis and the smoothness of the material gradation.
4. Satisfactory levels of accuracy can be obtained by applying the discrete layer model using a fairly small number of homogeneous layers. For the examples presented here, only 20 layers were required to achieve a maximum error of 5% relative to exact or converged solutions.
5. The approach presented here is not dependent on specific boundary conditions, although a higher number of layers and/or terms may be required to obtained accurate results.
6. For realistic material properties, the graded plate can result in smaller displacements and stresses, showing the advantage of using functionally graded materials. A reduction of 25% in the vertical displacement and about 20% in the in-plane normal stresses was obtained for the SSSS graphite/epoxy laminate by using the graded configuration instead of the homogeneous plate.
7. Use of functionally graded configurations eliminates the mismatch in the gradient of the displacements seen in plates with laminate made of different materials, and a considerable reduction of interlaminar/in-plane stresses at free edges is likewise expected.

Encouraged by the excellent results obtained here, and the fact that the present model usually results in smaller systems of equations to be solved in comparison to finite elements [25,26], the authors are currently working on the application of the proposed model to the solution of the dynamic analysis of functionally graded elastic, piezoelectric, and magnetostrictive plates.

References

[1] Kieback B, Neubrand A, Riedel H. Processing techniques for functionally graded materials. Mater Sci Eng A-Struct Mater Prop Microstruct Process 2003;362(1–2):81–105.

[2] Mortensen A, Suresh S. Functionally graded metals and metal-ceramic composites 1. Processing. Int Mater Rev 1995;40(6):239–65.

[3] Biesheuvel PM, Verweij H. Calculation of the composition profile of a functionally graded material produced by centrifugal casting. J Am Ceram Soc 2000;83(4):743–9.

[4] Put S, Vleugels J, Van der Biest O. Microstructural engineering of functionally graded materials by electrophoretic deposition. J Mater Process Technol 2003;143:572–7 [Special issue].

[5] Shen ZJ, Nygren M. Laminated and functionally graded materials prepared by spark plasma sintering. Key Eng Mater 2002;206(2):2155–8.

[6] Groves JF, Wadley HNG. Functionally graded materials synthesis via low vacuum directed vapor deposition. Compos Part B-Eng 1997; 28(1-2):57–69.

[7] Reddy JN. Analysis of functionally graded plates. Int J Numer Meth Eng 2000;47:663–84.

[8] Xiao HT, Yue ZQ, Tham LG, et al. Stress intensity factors for penny-shaped cracks perpendicular to graded interfacial zone of bonded bi-materials. Eng Fract Mech 2005;72(1):121–43.

[9] Sutradhar A, Paulino GH. Symmetric Galerkin boundary element computation of T-stress and stress intensity factors for mixed-mode cracks by the interaction integral method. Eng Anal Boundary Elem 2004;28(11):1335–50.

[10] Jain N, Shukla A. Displacements, strains and stresses associated with propagating cracks in materials with continuously varying properties. Acta Mech 2004;171(1-2):75–103.

[11] Zhou ZG, Wang B, Yang LJ. Investigation of the behavior of an interface crack between two half-planes of orthotropic functionally graded materials by using a new method. JSME Int J Series A-Solid Mech Mater Eng 2004;47(3):467–78.

[12] Zhou ZG, Wang B. Two parallel symmetry permeable cracks in functionally graded piezoelectric/piezomagnetic materials under anti-plane shear loading. Int J Solids Struct 2004;41(16-17):4407–22.

[13] Cheng ZQ, Batra RC. Deflection relationships between the homogeneous Kirchhoff plate theory and different functionally graded plate theories. Arch Mech 2000;52:143–58.

[14] Cheng ZQ, Batra RC. Exact correspondence between eigenvalues of membranes and functionally graded simply supported polygonal plates. J Sound Vib 2000;229:879–95.

[15] Cheng ZQ, Batra RC. Three-dimensional thermoelastic deformations of a functionally graded elliptic plate. Compos: Part B 2000;31: 97–106.

[16] Vel SS, Batra RC. Three-dimensional analysis of transient thermal stresses in functionally graded plates. Int J Solids Struct 2003;40: 7181–96.

[17] Vel SS, Batra RC. Three-dimensional exact solution for the vibration of functionally graded rectangular plates. J Sound Vib 2004;272: 703–30.

[18] Sankar BV. An elasticity solution for functionally graded beams. Compos Sci Technol 2001;61(5):689–96.

[19] Martin PA, Richardson JD, Gray LJ, et al. On Green's function for a three-dimensional exponentially graded elastic solid. Proc R Soc London Ser A-Math Phys Eng Sci 2002;458(2024): 1931–47.

[20] Pan E. Exact solution for functionally graded anisotropic elastic composite laminates. J Compos Mater 2003;37(21):1903–19.

[21] Batra RC, Jin J. Natural frequencies of a functionally graded rectangular plate. J Sound Vib 2005;282(1–2):509–16.

[22] Reddy JN. Energy and variational methods in applied mechanics. New York: John Wiley and Sons; 1984.

[23] Reddy JN. Mechanics of laminated composite plates: theory and analysis. 2nd ed. Boca Raton, FL: CRC Press; 1997.

[24] Reddy JN. A generalization of displacement-based laminate theories. Commun Appl Numer Meth 1987;3:173–81.

[25] Heyliger PR, Pan E. Static fields in magnetoelectroelastic lamintes. AIAA J 2004;42(7):1435–43.

[26] Heyliger PR, Ramirez F, Pan E. Two-dimensional static fields in magnetoelectroelastic laminates. J Intell Mater Syst Struct 2004; 15(9–10):689–709.